

## Epitaxial growth of thermally stable cobalt films on Au(111)

**N. Haag, M. Laux, J. Stöckl, J. Kollamana, J. Seidel, N. Großmann, R. Fetzer, L. L. Kelly, Z. Wei, Benjamin Stadtmüller, M. Cinchetti, M. Aeschlimann**

### Angaben zur Veröffentlichung / Publication details:

Haag, N., M. Laux, J. Stöckl, J. Kollamana, J. Seidel, N. Großmann, R. Fetzer, et al. 2016. "Epitaxial growth of thermally stable cobalt films on Au(111)." *New Journal of Physics* 18 (10): 103054. <https://doi.org/10.1088/1367-2630/18/10/103054>.



PAPER • OPEN ACCESS

## Epitaxial growth of thermally stable cobalt films on Au(111)

To cite this article: N Haag *et al* 2016 *New J. Phys.* **18** 103054

View the [article online](#) for updates and enhancements.

You may also like

- [Complementary properties of multiphoton quantum states in linear optics networks](#)  
Jun-Yi Wu and Mio Murao
- [The Holst spin foam model via cubulations](#)  
Aristide Baratin, Cecilia Flori and Thomas Thiemann
- [Influence of thermal annealing on the morphology and magnetic domain structure of Co thin films](#)  
Muchan Li, Zhongzheng Tian, Xuemin Yu et al.



## PAPER

## Epitaxial growth of thermally stable cobalt films on Au(111)

N Haag<sup>1</sup>, M Laux<sup>1</sup>, J Stöckl<sup>1</sup>, J Kollamana<sup>1</sup>, J Seidel<sup>1</sup>, N Großmann<sup>1</sup>, R Fetzter<sup>1</sup>, L L Kelly<sup>1</sup>, Z Wei<sup>1,2</sup>,  
B Stadtmüller<sup>1,3</sup>, M Cinchetti<sup>4</sup> and M Aeschlimann<sup>1</sup><sup>1</sup> Department of Physics and Research Center OPTIMAS, University of Kaiserslautern, Erwin-Schroedinger-Strasse 46, 67663 Kaiserslautern, Germany<sup>2</sup> College of Material Science and Engineering, Chongqing University, 400044 Chongqing, People's Republic of China<sup>3</sup> Graduate School of Excellence Materials Science in Mainz, Erwin Schroedinger Straße 46, 67663 Kaiserslautern, Germany<sup>4</sup> Experimentelle Physik VI, Technische Universität Dortmund, 44221 Dortmund, GermanyE-mail: [bstadtmueller@physik.uni-kl.de](mailto:bstadtmueller@physik.uni-kl.de)**Keywords:** thin films, structure formation, spin-dependent valence band structure, chemical composition, ferromagnetic materialRECEIVED  
20 July 2016REVISED  
7 September 2016ACCEPTED FOR PUBLICATION  
26 September 2016PUBLISHED  
31 October 2016

Original content from this work may be used under the terms of the [Creative Commons Attribution 3.0 licence](https://creativecommons.org/licenses/by/3.0/).

Any further distribution of this work must maintain attribution to the author(s) and the title of the work, journal citation and DOI.



## Abstract

Ferromagnetic thin films play a fundamental role in spintronic applications as a source for spin polarized carriers and in fundamental studies as ferromagnetic substrates. However, it is challenging to produce such metallic films with high structural quality and chemical purity on single crystalline substrates since the diffusion barrier across the metal-metal interface is usually smaller than the thermal activation energy necessary for smooth surface morphologies. Here, we introduce epitaxial thin Co films grown on an Au(111) single crystal surface as a thermally stable ferromagnetic thin film. Our structural investigations reveal an identical growth of thin Co/Au(111) films compared to Co bulk single crystals with large monoatomic Co terraces with an average width of 500 Å, formed after thermal annealing at 575 K. Combining our results from photoemission and Auger electron spectroscopy, we provide evidence that no significant diffusion of Au into the near surface region of the Co film takes place for this temperature and that no Au capping layer is formed on top of Co films. Furthermore, we show that the electronic valence band is dominated by a strong spectral contribution from a Co 3d band and a Co derived surface resonance in the minority band. Both states lead to an overall negative spin polarization at the Fermi energy.

## 1. Introduction

The general interest in ferromagnetic thin films is based on their important role both for spintronic applications as well as for fundamental research in magnetism. On the one hand, in modern spintronic assemblies such as magnetic tunnel junctions, ferromagnetic thin films are used as source for spin polarized carriers which can subsequently be injected into non-magnetic materials [1–5]. The efficiency of this injection process determines the overall performance of the device and depends crucially on the structural epitaxy and the energy level alignment of the spin-polarized band structure across the interface. On the other hand, in studies focusing on the adsorption of inorganic and organic materials on ferromagnetic surfaces, fundamental insight into the growth properties and the spin-dependent interactions across adsorbate-ferromagnetic metal interfaces can only be obtained for surfaces with low defect concentrations and large atomically flat terraces. In addition, thin films can reveal a uniform magnetization which is crucial for experimental studies without spatial resolution.

Along these lines, many studies focused on the growth properties of ferromagnetic materials such as cobalt, nickel or iron on different noble metal surfaces [6–16]. A prototypical model system which has been studied extensively in the last decades is Co on Cu(001) [17–27]. On this noble metal surface, thin cobalt films do not grow in a hexagonal crystal structure as expected from Co bulk crystals, but in a face-centered cubic (fcc) phase with a 2% larger surface lattice constant than the Cu(001) surface [20]. This small mismatch between both lattices leads to the formation of a metastable tetragonally distorted fcc structure with surface orientation in (001) direction. The magnetic anisotropy is oriented in-plane with its uniaxial anisotropy axis along the [110]-direction of copper. Due to the well known structural and electronic properties of Co/Cu(001) films, this

material system has been exploited as ideal substrate, for example to study the interactions between organic or inorganic adsorbates and ferromagnetic surfaces [21–31]. In this respect, however, the low diffusion barrier of copper into the cobalt film makes Co/Cu(001) thin films grown at room temperature thermally unstable [23]. Thermal activation at 450 K results in an interdiffusion and intermixing of both elements [18, 32–35] which leads to a significant quenching of the magnetic properties of the Co films [33]. This is a strong drawback for the structural properties of such films since the formation of large terraces and smooth film morphologies requires thermal activation of surface diffusion. Similarly, thermal activation of surface diffusion and rotation is also necessary for (organic) adsorbates on ferromagnetic surfaces to ensure long range order in these adsorbate films.

In this paper we overcome these limitations by proposing Co/Au(111) as a thermally stable ferromagnetic thin film that can be grown at room temperature. We present a comprehensive study of the structural, electronic and spin-dependent properties of thin Co films grown on a Au(111) surface. The studies have been conducted by scanning tunneling microscopy (STM), low-energy electron diffraction (LEED), Auger electron spectroscopy (AES), x-ray photoelectron spectroscopy (XPS), and spin-resolved photoemission spectroscopy (SR-PES).

The morphology of as-grown and annealed Co/Au(111) films was investigated by STM for two Co coverages of 8 and 20 monolayers (ML) which corresponds to 16 and 40 Å, respectively. After Co deposition at room temperature, Co forms small islands with an average size smaller than 120 Å. These islands are transformed into atomically flat terraces with average size of up to 500 Å by sample annealing at 575 K for at least 10 min. This observation clearly underlines the necessity of thermally induced surface diffusion to obtain high quality Co films. Subsequently, our LEED studies reveal the growth behavior of Co/Au(111) as a function of the Co film thickness after sample annealing to 575 K. After an initially pseudomorphic growth of Co on Au(111), clear indications of a structural transition to a hexagonal crystal structure with a surface lattice constant similar to the (0001) oriented surface of Co single crystals could be observed starting from 4 ML coverage. Above a coverage of 4 ML Co, the surface exhibits large monoatomic terraces. By using AES and XPS we are able to monitor Au contamination within the Co layer which allows us to exclude diffusion from Au into the thin Co-film for the sample annealing procedure applied in all our experiments, i.e., 575 K for 10 min. This indicates a higher thermal stability of Co/Au(111) compared to the model system Co/Cu(001) [18, 32–35] which is high enough to thermally activate the formation of ordered adsorbate overlayers on this ferromagnetic surface. Finally, our spin-resolved photoelectron spectroscopy experiments are used to characterize the valence electronic and spin-dependent properties of these films. We found clear signs of a surface resonance in the minority band structure which results in a negative spin polarization of the valence electrons at the Fermi level.

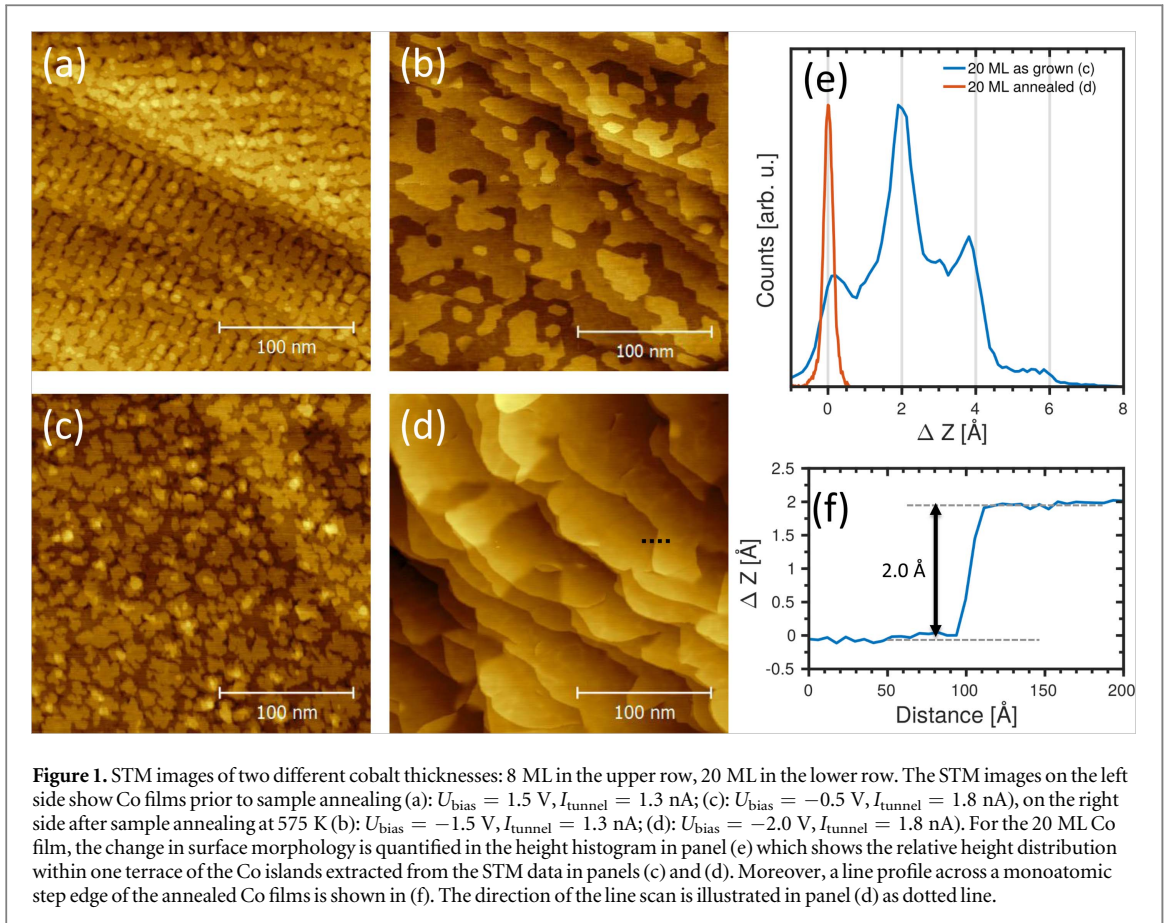
## 2. Experimental setup

All sample preparations were performed in an ultra-high vacuum (UHV) environment with base pressures lower than  $2 \times 10^{-10}$  mbar. The surface of a (111)-oriented gold crystal was cleaned by repeated cycles of argon ion bombardment and subsequent annealing at a temperature of 805 K. This procedure is known to result in well-ordered surfaces with large terrace widths of approx. 500 Å [36]. The Au(111) surface also showed sharp diffractions spots of the  $22 \times \sqrt{3}$  herringbone reconstruction [37] visible up to the third order. Subsequently, cobalt films were evaporated onto a clean Au(111) surface by electron beam epitaxy using a commercial evaporator (FOCUS EFM3). All Co films were grown at room temperature. The Co coverage was determined by deposition rate and time, monitored with a quartz micro balance and confirmed by the attenuation of dedicated substrate signals in AES and XPS. Structural characterization of the Co films was performed by LEED using a 3-grid SpectraLEED system (Omicron). As a complementary method the surface structure and roughness was also determined by scanning tunneling microscopy (STM) experiments using an Omicron VT-AFM XA system. All STM data were recorded in the constant current mode at room temperature.

The valence band structure of the films was characterized by ultraviolet photoemission spectroscopy (UPS) using a hemispherical analyzer (SPECS 150) and monochromatic He-I radiation ( $h\nu = 21.2$  eV) of a gas discharge source. Additionally, spin-resolved photoemission experiments (SR-PES) were carried out with a commercial cylindrical sector analyzer (Focus CSA 300) exhibiting an energy resolution of 420 (210) meV at pass energy of 8 (4) eV for He-I radiation (UV laser radiation) and an acceptance angle of  $\pm 13^\circ$ . The spin-resolved photoemission yield was detected with a SPLEED analyzer (FOCUS) mounted after the CSA energy analyzer. The energy dependent spin polarization  $P(E)$  is determined from the experimental signals as

$$P = \frac{1}{S} \frac{\sqrt{I_{1A} \cdot I_{2B}} - \sqrt{I_{2A} \cdot I_{1B}}}{\sqrt{I_{1A} \cdot I_{2B}} + \sqrt{I_{2A} \cdot I_{1B}}}$$

where  $S = 0.2$  is the spin sensitivity factor (Sherman factor).  $I_{1A/B}$  and  $I_{2A/B}$  are the experimental signals recorded with the SPLEED detector for two opposite sample magnetization directions A/B. This data acquisition procedure allows us to remove the instrumental asymmetry of the detector. The spin-polarized photoemission



spectra are obtained from the spin polarization by

$$I_{\uparrow/\downarrow} = I_0 \cdot (1 \pm P)$$

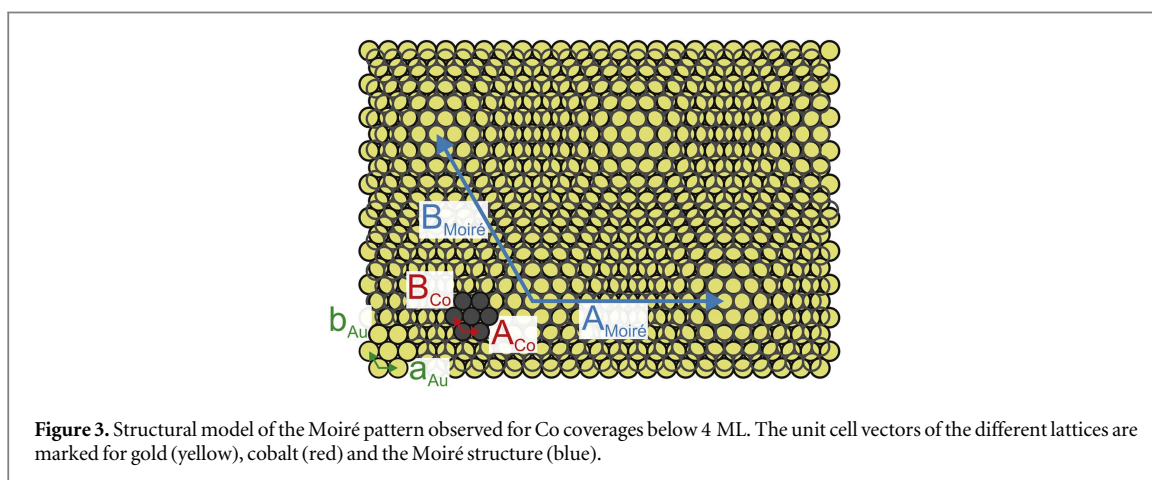
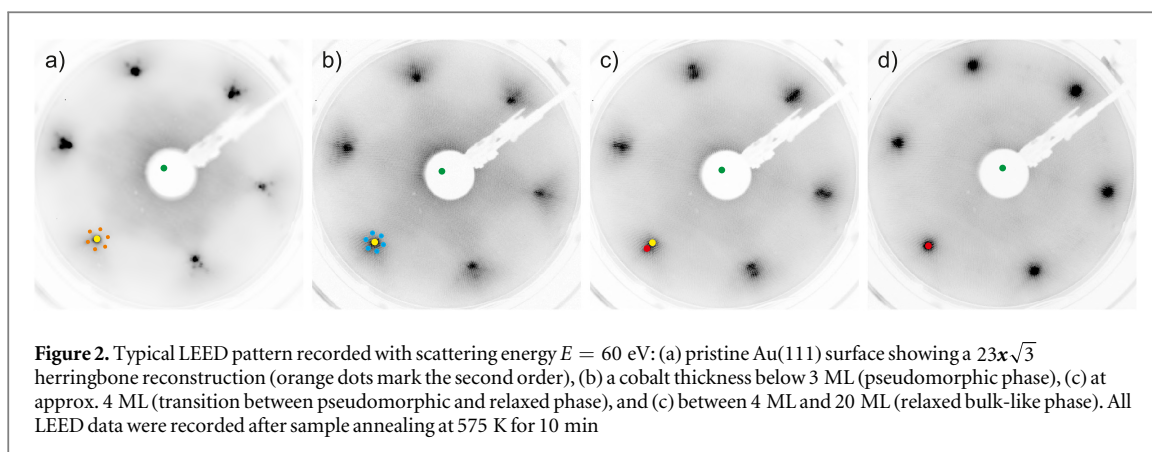
where  $I_0$  is the spin-integrated average photoemission intensity. (ArrowUp) and (ArrowDown) indicate majority and minority electrons, respectively.

The chemical composition of the thin Co/Au(111) films was determined using XPS and AES. All XPS measurements were performed using linear polarized synchrotron radiation with a photon energy of 420 eV at the NanoESCA endstation of the Elettra synchrotron radiation facility in Trieste, Italy.

### 3. Growth, morphology and chemical composition of Co films on Au(111)

First, we discuss the morphology and surface roughness of the Co films grown on Au(111) as investigated by STM at room temperature. In the STM studies, we have considered two Co nominal coverages: 8 ML (figures 1(a) and (b)) and 20 ML (figures 1(c) and (d)). Figures 1(a) and (c) show large-scale STM images of the as deposited 8 ML and 20 ML Co. The 8 ML film consists of Co islands with average size of 80 Å. These islands are arranged in stripes with an average distance of 120 Å. The stripes are rotated by 120° with respect to each other and follow the orientation of the gold herringbone reconstruction. In agreement with previous studies [38–40], we expect that Co starts to nucleate at the elbows of the Au reconstruction and subsequently forms linear rows of Co islands. These findings again demonstrate the strong influence of the Au(111) surface on growth properties for thin Co films. In contrast, the morphology of the high coverage Co film is dominated by randomly arranged islands with a slightly larger average size of 150 Å. For these films, the influence of the Au(111) surface on the morphology of the as-grown Co film is significantly reduced which leads to the absence of any preferential orientations of the Co islands.

The morphology of the Co films changes significantly for both coverages after thermal activation, i.e., after sample annealing at 575 K for 45 min. Instead of small islands, atomically flat terraces with a step height of 2 Å (see figure 1(f)) are observed as illustrated in the corresponding STM images in figures 1(b) and (d), respectively. The average size of these terraces is at least 500 Å and therefore comparable to typical terraces of metal single crystal surfaces. The surface roughness can be estimated from the height histogram plots from figure 1(e) and yields a root mean square (RMS) value of 1.4 Å and 0.16 Å for the 20 ML film prior and after sample annealing at

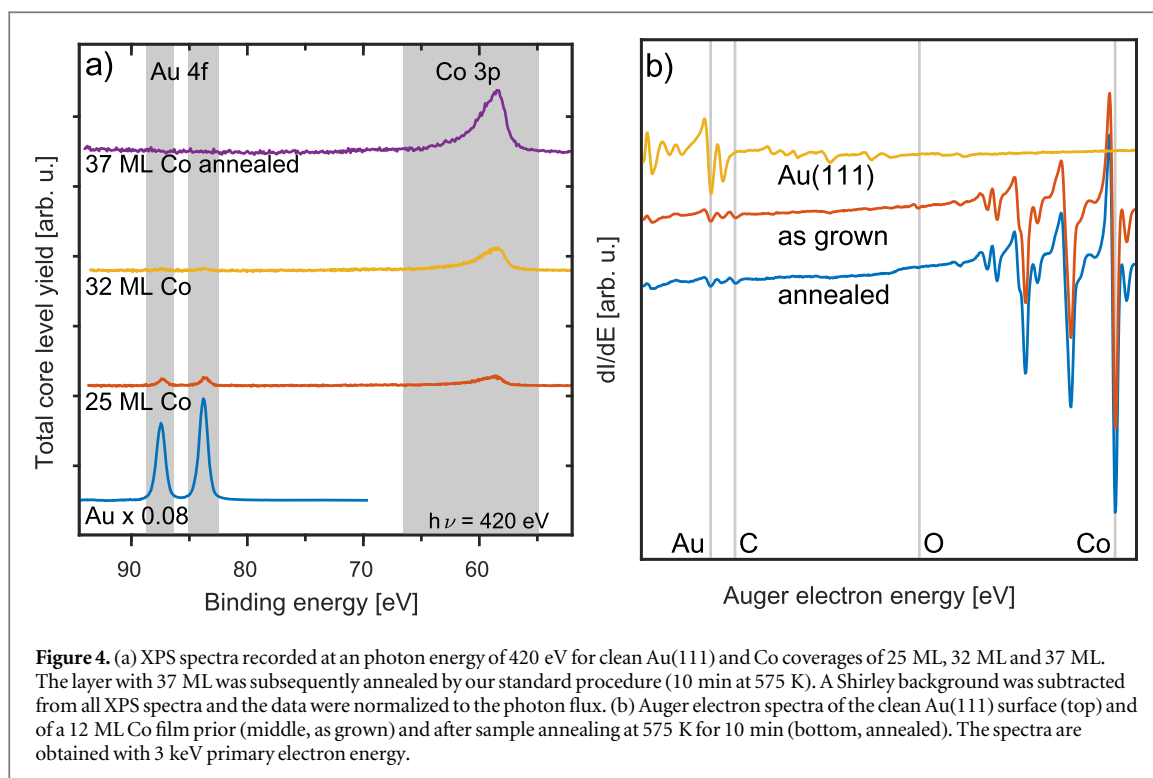


575 K, respectively. A direct comparison between figures 1(b) and (d) reveals that the Co terraces are slightly larger for Co films with higher coverages. These STM investigations clearly show the necessity of sample annealing up to 575 K to produce high quality Co films on Au(111) with large atomically flat terraces. While similar changes in surface morphology were also reported for ultrathin ferromagnetic films grown on different single crystalline surfaces such as Ru(0001) [41] and Fe(001) [42], our results show that this thermal activation procedure can also be extended to bulk-like ferromagnetic films.

Moreover, the shape of the islands edges is different for both coverages. For the low Co coverage film, the terraces show sharp and straight edges that are oriented along high symmetry directions of the gold substrate. This indicates that the formation of atomically flat islands is still determined by the structure and morphology of the Au(111) surface and its surface reconstruction. When increasing the Co thickness, the island edges become smooth and curved. This transition must be attributed to the reduced influence of the Au(111) surface. Instead, the shape of the Co islands must be the result of an optimization of the free energy of the Co surface. In addition, the step height of 2.0 Å observed for the 20 ML Co film matches the expected value for the spacing between two Co planes of a bulk crystal and hence also points to the formation of bulk-like Co films which are no longer influenced by the Au substrate.

At this point, it is also important to note that we do not observe any indications for an Au capping of the Co films studied with STM. In particular, there are no signs for the formation of locally ordered surface superstructures or even of a herringbone-like surface reconstruction as known for hexagonal Au surfaces. Although STM is not the ideal experimental tool to study chemical compositions of surfaces, these results are a first hint that Au atoms do not accumulate on the Co surface and do not form a closed Au capping layer.

After this initial discussion of the surface morphology, we now discuss the growth behavior of Co on Au(111) as investigated by LEED. Depending on the Co coverage, the LEED diffraction patterns shown in figure 2 reveal three different crystalline structures. Figure 2(a) shows the LEED pattern of the pristine Au(111) surface with a hexagonal pattern with six bright and narrow diffraction maxima. Figure 2(b) shows the LEED pattern of a thin Co film with coverage below 3 ML. The radial position of the first order diffraction spots still corresponds to the surface lattice constant of the bare gold surface (2.88 Å). A closer look at figure 2(b) shows that each of the six diffraction maxima is surrounded by six satellite peaks that are also arranged in a hexagonal pattern (indicated by



blue dots in figure 2(b)). Most intriguing, this hexagonal arrangement is rotated by  $30^\circ$  with respect to the satellite diffraction maxima of the bare Au(111) surface (orange dots in figure 2(a)) and hence cannot be explained by a preferred growth of Co along the Au herringbone reconstruction. Instead, these diffraction spots can be attributed to a hexagonal superstructure with a periodicity of  $31.5 \pm 2.7 \text{ \AA}$  and an azimuthal orientation similar to the hexagonal grid of the bare gold surface. Within the experimental uncertainty, this superstructure matches the Moiré structure which was already reported for ultrathin ( $<4 \text{ ML}$ ) Co films on Au(111) by Cagnon *et al* [43]. In this coverage regime, they proposed that Co forms a commensurate superstructure with 11 Co atoms per 10 gold surface atoms as shown in the real space model of the Moiré structure in figure 3(a).

For a Co coverage of 4 ML (figure 2(c)), we observe six additional diffraction maxima with similar azimuthal orientation but larger distance from the center of the surface Brillouin zone than in figure 2(b). The radial position of these diffraction maxima points to a surface lattice constant of  $2.7 \pm 0.2 \text{ \AA}$ . This value is slightly smaller compared to the lattice constant of the clean Au(111) surface ( $2.88 \text{ \AA}$ ) and indicates that Co grows in a hexagonal structure with slightly smaller unit cell vectors. The smaller unit cell size is expected due to the smaller size of Co atoms compared to Au atoms. For Co coverage above 4 ML (figure 2(d)), only the new diffraction features can be observed while the ones of the initial Co film are completely attenuated. The lattice constant of this new hexagonal structure is  $2.5 \pm 0.2 \text{ \AA}$  and hence almost identical to the surface lattice constant of the corresponding cut through a Co bulk crystal [44]. This clearly shows that beyond a critical Co coverage of 4 ML, Co grows in a relaxed structural phase that is no longer influenced by the Au(111) lattice. In addition, all diffraction features of equal diffraction order show an identical intensity modulation depending on the electron scattering energy, proving a hexagonal stacking order of Co layers in our films, in good agreement with previous studies [45]. This conclusively shows that the crystalline structure and the structural surface properties of thin Co films undergoes a transition from pseudomorphic growth with a larger lattice constant up to 4 ML coverages to a relaxed growth mode that is structurally identical to the Co(0001) surface of a single crystal. For Co coverages larger than 20 ML, no further changes could be observed.

The chemical composition of as grown and annealed (575 K for 10 min) Co films on Au(111) was investigated by x-ray photoemission spectroscopy (XPS) and Auger electron spectroscopy (AES). To determine the surface termination and the chemical composition of the Co/Au films, XPS spectra were recorded in the binding energy range from 45 eV up to 93 eV for different Co coverages (figure 4(a)). This energy region includes the Au 4f as well as the Co 3p core levels and enables us to monitor signals of the substrate and adsorbate material. For increasing Co coverage, the signal of the Au 4f levels is continuously attenuated while the Co 3p signal increases almost exponentially with coverage. Most importantly, the Au signal is completely suppressed for the largest cobalt coverage of 37 ML which does not change even after subsequent annealing. This allows us to rule out a gold contamination within a probing depth of 50  $\text{\AA}$ . The latter value was estimated by assuming a reduction of the Au 4f signal below 1% of the initial intensity and an electron mean free path of approximately

10 Å [46] for the given kinetic energy. This result provides clear evidence that no additional gold adlayer is formed as capping layer on top of epitaxial cobalt film grown on Au(111).

In addition, the Auger electron spectra of the as-grown and the annealed sample are shown in figure 4(b) together with the reference spectrum of the clean Au(111) surface. The AES signal of the as-grown Co film (center line in figure 4(b)) is dominated by two sets of Auger peaks: the Co LMM peaks in the energy range between 600 eV and 800 eV, and the Au NOO peaks between 150 eV and 300 eV. The latter peaks exhibit a very low intensity and are clearly attenuated compared to the AES signal of the clean Au(111) surface (top line). A detailed analysis of the peak-to-peak amplitudes of the Auger signals including energy dependent sensitivity factors for each element [47] resulted in the following chemical composition of the surface region of the Co/Au film: 79% cobalt (775 eV), 19% gold (239 eV), 2% carbon (272 eV) and <1% oxygen (503 eV). The latter two species are due to a minor contamination of our sample during the evaporation procedure. The same analysis of the spectra of the sample annealed at 575 K for 10 min (bottom line) reveals a chemical composition of 84% cobalt and 14% gold. The carbon contamination stays constant at a value of 2%. The presence of the Au NOO signal is not surprising when considering the 12 ML coverage of the Co film. In analogy to the discussion of core level data above, the probing depth for electrons of the Au NOO signal at 239 eV can be estimated to be 42 Å [46]. Hence, the remaining intensity of 19% and 14% arises from the gold substrate underneath the cobalt film. The reduction of the Au signal by the annealing procedure is in good agreement with the morphology changes observed in the STM data in figure 1 that suggest a flattening of the Co islands. Furthermore the results prove the absence of an Au covering layer or superstructure on top of the Co film as such a layer would produce a large signal independent of the film thickness for the Au related peaks in both the AES and the XPS measurements.

In conclusion, our XPS and AES studies provide clear evidence for the thermal stability of the chemical composition of the thin Co films during our sample annealing procedure even for the buried interface between Au(111) and the cobalt layer.

The effect of diffusion of substrate atoms into magnetic films is also heavily discussed in the literature. Speckmann *et al* [48] observed clear indications for Au diffusion into ultrathin Co films with Co coverages between 2–4 ML. We believe that these results are not in contradiction to our study of Co(0001) films with film coverages beyond 12 ML. However, we can speculate that the effect of interdiffusion of Au into Co is more crucial for thin Co films since the activation of surface diffusion is significantly smaller than for bulk diffusion [32]. Therefore for thicker films, the thermal activation energy at 575 K is not high enough to trigger a significant diffusion of Au into the Co bulk. This can explain the different conclusion of our work and the study of Speckmann *et al* [48] regarding the thermal stability of thin Co films on Au(111).

#### 4. Electronic and spin-dependent properties of thin Co(0001) films

After the detailed characterization of the growth behavior and the chemical composition of thin Co films on Au(111), we now focus on their electronic and spin-dependent properties as studied by ultraviolet photoemission spectroscopy (UPS) and spin-resolved photoelectron spectroscopy (SR-PES). The left panel of figure 5 shows UPS spectra with increasing Co coverage (top to bottom), recorded in normal emission geometry. All spectra of thin Co films show a clear spectroscopic feature arising close to the Fermi level, which can be attributed to 3d bulk bands of the Co film. A similar peak has also been reported for thin Co films on Cu(001) [19, 49]. The photoemission maxima at larger binding energies (between 3.9 eV and 6.1 eV) can be assigned to the Au 5d bands that are continuously damped for increasing Co coverage. A quantitative evaluation of the peak area of the Au bands yields a clear exponential behavior with a decay rate that matches the electron mean free path of approximately 3.5 ML [46]. This exponential reduction of the Au signal supports again the suggested layer-by-layer growth of the Co films in agreement with our previous STM studies. Sample annealing does not alter the spectroscopic shape of the Co valence band structure (last graph in figure 5(a)). In accordance with all previous results, these photoemission data clearly support our statement of the large stability of thin Co films during the sample annealing procedure.

More insight into the magnetic properties can be obtained by spin-resolved PES. The 20 ML Co(0001) film was magnetized in remanence along the  $[\bar{1}100]$  direction by an external magnetic field of 10 mT. This leads to an uniform in-plane saturation magnetization of the Co film in the absence of an external magnetic field [33]. The photoemission spectra of the minority and majority spin channel are shown in figure 5(b) as red and blue lines.

The spin resolved photoemission spectra in figure 5(b) show a clear 3d bulk signal in both spin channels with highest spectral intensity at a binding energy of 0.9 eV, but with a significantly different spectral shape. In addition, a sharp spectroscopic feature can be observed close to the Fermi energy in the minority spin channel that is not present in the majority spin channel. These differences are directly reflected in the spectroscopic features of spin polarization in figure 5(c). In the binding energy range above 4 eV (i), a constant spin-

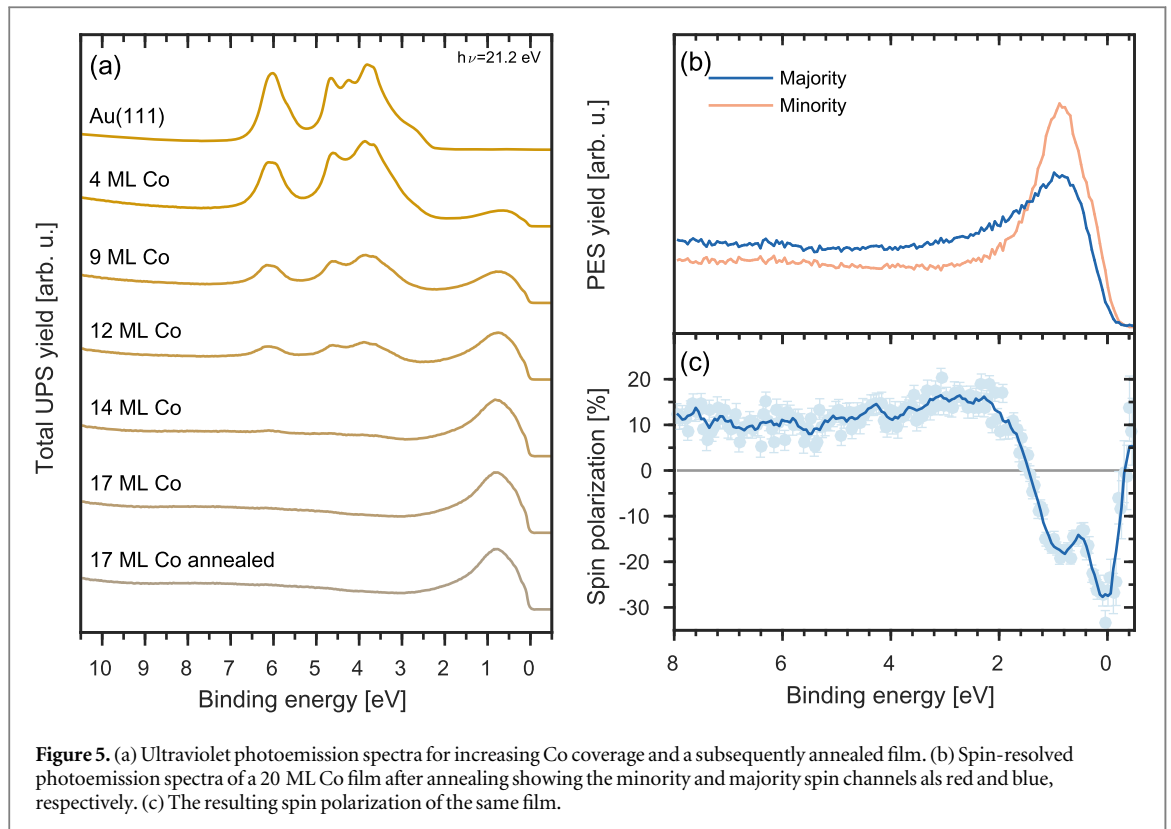


**Figure 5.** (a) Ultraviolet photoemission spectra for increasing Co coverage and a subsequently annealed film. (b) Spin-resolved photoemission spectra of a 20 ML Co film after annealing showing the minority and majority spin channels as red and blue, respectively. (c) The resulting spin polarization of the same film.

polarization of around +10% is found. Closer to the Fermi energy, the spin-polarization first reveals a broad maximum at 2.8 eV (ii), and subsequently decreases to negative values up to  $-30\%$ .

A similar shape of the spin-polarization was already reported for thin Co(0001) films [50, 51] and even for Co(001) films on Cu(001) [19, 49]. In our case, however, the spin-polarization does not only reveal one broad dip close to the Fermi energy as reported before [21, 22, 52], but consists of two distinct features. The first dip at 0.9 eV below  $E_F$  coincides with the intense peak in the spin resolved photoemission spectra in figure 5(b), while the second dip at 0.3 eV below  $E_F$  does not correspond to any characteristic spectral intensity in the photoemission spectra. Yet we attribute this band to the surface resonance of the Co(0001) surface.

This is in accordance with high resolution angle resolved photoemission studies which already reported the existence of a surface resonance with small energy dispersion for hcp Co films [12, 53]. This also matches with theoretical studies of Co(0001) predicting the existence of a surface state or resonance at the  $\Gamma$ -point of the surface Brillouin zone [54]. At this point, it should be mentioned that our experimental findings for the entire spin polarized valence band structure fits also perfectly to previous theoretical efforts performed for Co(0001) [54]. This underlines the similarity between thin Co(0001) films with coverages beyond 20 ML and Co bulk crystals.

In order to confirm the existence of a surface resonance with minority spin character in the photoemission spectra of the Co(0001) films at 0.3 eV below  $E_F$ , we also performed spin-resolved PES experiments using the fourth harmonic of a femtosecond laser system as excitation source. Figure 6(a) displays the spin-resolved photoemission spectra and the corresponding spin polarization recorded in normal emission geometry with p- and s-polarized laser light. The most striking difference between the SR-PES data for p- and s-polarized light occurs in the minority spin channel. Here, a distinct maximum is visible at  $-0.3$  eV for excitation with p-polarized light, while it is absent for excitation with s-polarized light. Considering the polarization selection rules for normal emission geometry, only p-polarized light, i.e., light with an electric field vector component perpendicular to the surface, can excite initial states with  $\Delta_1$  (highest azimuthal) symmetry such as surface resonances with orbital wave functions perpendicular to the surface, i.e., exhibiting  $p_z$  or  $d_z$  orbital character. These states will hence not contribute to the photoemission intensity when excited with s-polarized light, i.e., light with an electric field vector oriented parallel to the surface. Therefore, we can conclude that the peak in the minority photoemission spectrum for p-polarized light is due to a surface resonance with minority spin and  $d_z$  orbital character, in agreement with a previous spin polarized STS study on Co(0001) [55]. This state is hence responsible for the negative peak in the spin-polarization at 0.3 eV below  $E_F$  (see figures 5(c) and 6(a)). The existence of a surface state is also a strong indication for a contamination free surface and hence provides further evidence that the Co regions close to the surface is not contaminated by diffusion of Au atoms.

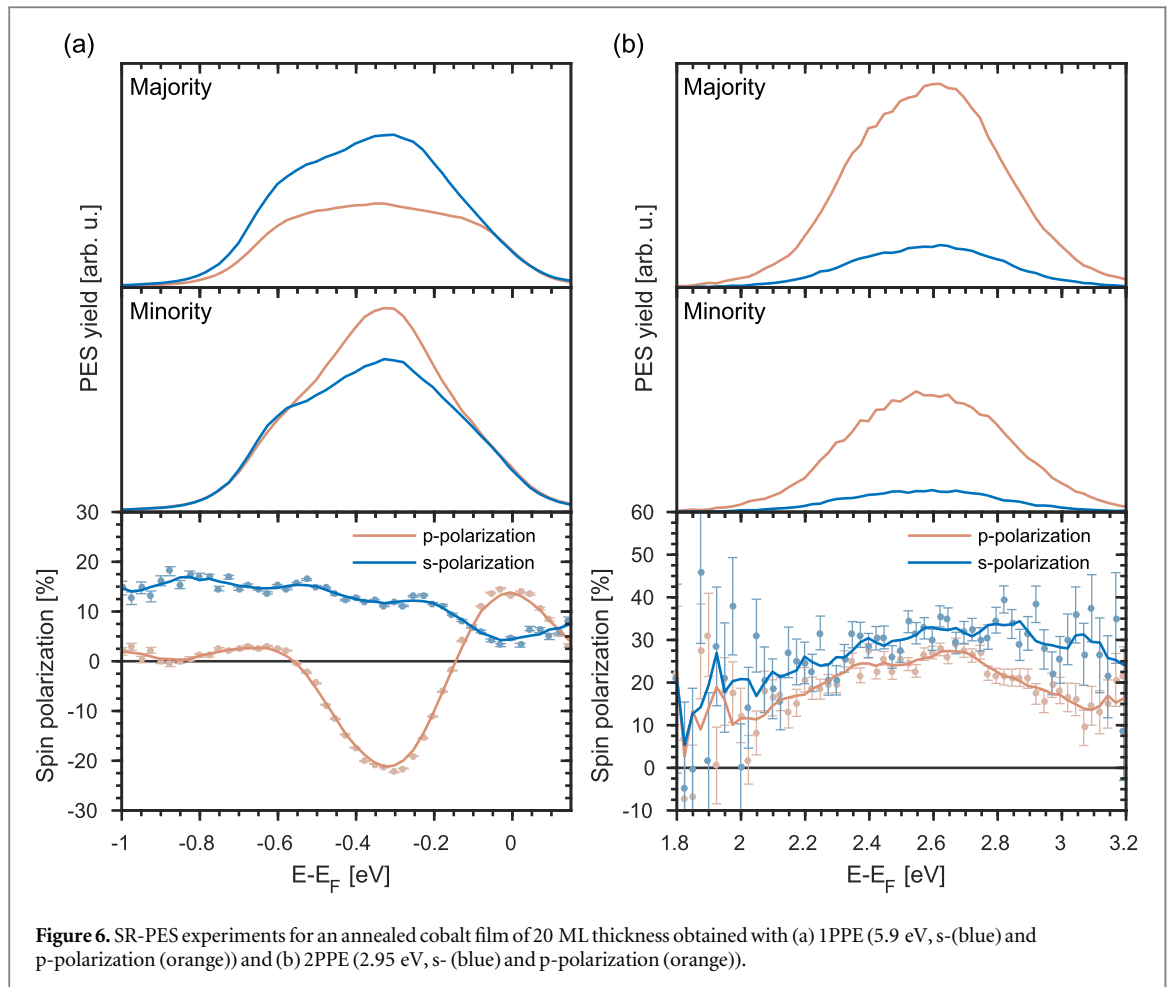


**Figure 6.** SR-PES experiments for an annealed cobalt film of 20 ML thickness obtained with (a) 1PPE (5.9 eV, s- (blue) and p-polarization (orange)) and (b) 2PPE (2.95 eV, s- (blue) and p-polarization (orange)).

The spin polarization determined with s-polarized light (blue line in figure 6(a)) is positive in the entire energy range and decreases continuously from 15% at  $-1.0$  eV to 5% right at the Fermi level. This is different compared to the negative spin-polarization found in the entire binding energy between 2 eV and the Fermi level in the VUV-PES data of figure 5(c). This discrepancy can be attributed to the photoemission process itself, as different electronic transitions for different photon energies lead to different experimental spin polarizations. However, since final state effects are more crucial for low photon energies used in laser spectroscopy, we speculate that the experimental spin polarization determined by VUV excitation is dominated by the spin-polarization of the initial state while the one obtained with laser excited is strongly influenced by final state effects. Note that a similar effect was observed for the model system Co/Cu(001). For this ferromagnetic surface, a positive spin polarization was reported for the occupied valence states using laser based excitations even though theoretical calculations predicted a negative spin polarization of the 3d states close to the Fermi level [18].

This effect is even enhanced in the spin-resolved two-photon photoemission (2PPE) spectra shown in figure 6(b), again recorded for p- and s-polarized laser light (photon energy 3.1 eV). 2PPE is sensitive not only to the initial and final state, but also to the intermediate state between the Fermi and the vacuum energy populated during the 2PPE process [56]. The spectra in figure 6(b) show a rather similar shape with no distinct maxima, pointing to the absence of unoccupied bands with large density of states in this energy range. In addition, no significant difference can be observed for p- and s-polarized excitation which indicates the absence of any unoccupied surface state. As a result, the spin polarization is almost identical in both cases and shows an almost constant value of around 25% over the complete spectral range. This spin-polarization is significantly larger than the one obtained by 1PPE. This effect is also well known for the model system Co/Cu(001). In analogy to the latter case, we attribute this behavior to the spin-filtering effect in the 2PPE process resulting from the spin-dependent electron scattering rates in the intermediate state [56, 57].

## 5. Summary

In conclusion, we have investigated the initial growth behavior of epitaxial Co films on an Au(111) single crystal surface by LEED and STM. Below Co coverages of 8 ML, the ultrathin Co films still reflect the influence of the Au(111) substrate. Besides a pseudomorphic growth for coverages below 3 ML, the edges of the Co islands follow high symmetry directions and steps of the Au(111) substrate even after thermal activation. Beyond coverages of 20 ML, the properties of thin Co films on Au(111) are identical to the ones of a Co bulk crystal. The surface reveals a hexagonal surface unit cell identical to the Co(0001) surface of a Co bulk crystal with large terraces of 500 Å average size.

Moreover, the spin-dependent electronic properties of such a bulk-like Co film are also identical to a Co bulk crystal as revealed by SR-PES. The valence band structure is dominated by the Co 3d bands with dominant density of states in the minority spin signal close to  $E_F$ . Besides the Co 3d bands, we could identify a surface resonance close to the Fermi level which leads to a second negative dip in the spin polarization curve. All these findings lead to the conclusion that the geometric, electronic and spin-dependant properties of epitaxial Co films on Au(111) are identical to the ones of a Co single crystal.

Most importantly, we were also able to provide clear evidence of the thermal stability of bulk-like Co films up to sample annealing temperatures of 575 K. The chemical composition of the Co films does not indicate the formation of an Au capping layer on top of the Co films. In addition, the chemical composition is not significantly altered by sample annealing cycles which points to a negligible diffusion of Au atoms into the Co film for sample annealing temperatures up to 575 K. This has consequences for the surface morphology of the Co film which is significantly improved by sample annealing at high sample temperature. Moreover, the high thermal stability of thin Co/Au(111) films makes this epitaxial Co-substrate highly interesting for fundamental studies of interfaces formed between non-magnetic metals and ferromagnetic Co or between organic adsorbates and ferromagnetic Co. For the latter case, thermally activated diffusion or rotation of (organic) adsorbates on ferromagnetic surfaces becomes possible without contaminating the ferromagnetic substrate. This will be a vital step on the route to fabricate ordered organic adsorbate layers on ferromagnetic surface, as recently shown by Kollamana et al [58].

## Acknowledgments

The research leading to these results was financially supported by the German Science foundation (DFG) via the SFB/TRR 88 3MET, the SFB/TRR 173 Spin + X: spin in its collective environment (Projects A02 and B05) and the Carl-Zeiss-Stiftung. BS thankfully acknowledge financial support from the Graduate School of Excellence MAINZ (Excellence Initiative DFG/GSC 266).

## References

- [1] Moodera J S and Mathon G 1999 Spin polarized tunneling in ferromagnetic junctions *J. Magn. Magn. Mater.* **200** 248–73
- [2] Yuasa S, Nagahama T, Fukushima A, Suzuki Y and Ando K 2004 Giant room-temperature magnetoresistance in single-crystal Fe/MgO/Fe magnetic tunnel junctions *Nat. Mater.* **3** 868–71
- [3] Djayaprawira D D, Tsunekawa K, Nagai M, Maehara H, Yamagata S, Watanabe N, Yuasa S, Suzuki Y and Ando K 2005 230% room-temperature magnetoresistance in CoFeB/MgO/CoFeB magnetic tunnel junctions *Appl. Phys. Lett.* **86** 092502
- [4] Žutić I and Das Sarma S 2004 Spintronics: fundamentals and applications *Rev. Mod. Phys.* **76** 323–410
- [5] Wolf S A, Awschalom D D, Buhrman R A, Daughton J M, von Molnár S, Roukes M L, Chtchelkanova A Y and Treger D M 2001 Spintronics: a spin-based electronics vision for the future *Science* **294** 1488–95
- [6] Wuttig M, Feldmann B, Thomassen J, May F, Zillgen H, Brodde A, Hannemann H and Neddermeyer H 1993 Structural transformations of fcc iron films on Cu(100) *Surf. Sci.* **291** 14–28
- [7] Schmid A K and Kirschner J 1992 *In situ* observation of epitaxial growth of Co thin films on Cu(100) *Ultramicroscopy* **42–44** 483–9
- [8] Osterwalder J 2001 Correlation effects and magnetism in 3d transition metals *J. Electron Spectros. Relat. Phenomena* **117–118** 71–88
- [9] Sawada M, Hayashi K and Kakizaki A 2003 Perpendicular magnetic anisotropy of Co/Pd(111) studied by spin-resolved photoelectron spectroscopy *J. Phys. Soc. Japan* **72** 1161–5
- [10] Wasniowska M, Janke-Gilman N, Wulfhekel W, Przybylski M and Kirschner J 2007 Growth and morphology of Cobalt thin films on Pd(111) *Surf. Sci.* **601** 3073–81
- [11] Getzlaff M, Bansmann J, Braun J and Schönhense G 1996 Spin resolved photoemission study of Co(0001) films *J. Magn. Magn. Mater.* **161** 70–88
- [12] Wetli E, Kreuz T, Schmid H, Greber T, Osterwalder J and Hochstrasser M 1998 High-resolution photoemission study of hcp-Co(0001) *Surf. Sci.* **402–404** 551–5
- [13] Meyer J A, Baikie I D, Kopatzki E and Behm R J 1996 Preferential island nucleation at the elbows of the Au(111) herringbone reconstruction through place exchange *Surf. Sci.* **365** L647–51
- [14] Kowalczyk P, Kozłowski W, Klusek Z, Olejniczak W and Datta P K 2007 STM studies of the reconstructed Au(111) thin-film at elevated temperatures *Appl. Surf. Sci.* **253** 4715–20
- [15] Oepen H P, Millev Y T and Kirschner J 1997 The reorientation transition in Co/Au(111) *J. Appl. Phys.* **81** 5044
- [16] Allenspach R, Stamparoni M and Bischof A 1990 Magnetic domains in thin epitaxial Co/Au(111) films *Phys. Rev. Lett.* **65** 3344–7

- [17] Kief M T and Egelhoff W F 1993 Growth and structure of Fe and Co thin films on Cu(111), Cu(100), and Cu(110): a comprehensive study of metastable film growth *Phys. Rev. B* **47** 10785–814
- [18] Andreyev O et al 2006 Spin-resolved two-photon photoemission study of the surface resonance state on Co/Cu(001) *Phys. Rev. B* **74** 195416
- [19] Schmid A K, Atlan D, Itoh H, Heinrich B, Ichinokawa T and Kirschner J 1993 Fast interdiffusion in thin films: scanning-tunneling-microscopy determination of surface diffusion through microscopic pinholes *Phys. Rev. B* **48** 2855–8
- [20] De Miguel J J, Cebollada A, Gallego J M, Ferrer S, Miranda R, Schneider C M, Bressler P, Garbe J, Bethke K and Kirschner J 1989 Characterization of the growth processes and magnetic properties of thin ferromagnetic cobalt films on Cu(100) *Surf. Sci. Lett.* **211–212** A143
- [21] de Miguel J J, Cebollada A, Gallego J M, Miranda R, Schneider C M, Schuster P and Kirschner J 1991 Influence of the growth conditions on the magnetic properties of fcc cobalt films: from monolayers to superlattices *J. Magn. Magn. Mater.* **93** 1–9
- [22] Schneider C M, Bressler P, Schuster P, Kirschner J, de Miguel J J and Miranda R 1990 Curie temperature of ultrathin films of fcc-cobalt epitaxially grown on atomically flat Cu(100) surfaces *Phys. Rev. Lett.* **64** 1059–62
- [23] Allmers T and Donath M 2011 Controlling Cu diffusion in Co films grown on Cu(001) *Surf. Sci.* **605** 1875–80
- [24] Cerda J R, Andres P L D, Cebollada A, Miranda R, Navas E, Schuster P, Schneider C M and Kirschner J 1993 Epitaxial growth of cobalt films on Cu(100): a crystallographic LEED determination *J. Phys.: Condens. Matter* **5** 2055–62
- [25] Clemens W, Vescovo E and Kachel T 1992 Spin-resolved photoemission study of the reaction of O<sub>2</sub> with fcc Co(100) *Phys. Rev. B* **46** 4198–204
- [26] Schmidt A B, Pickel M, Allmers T, Budke M, Braun J, Weinelt M and Donath M 2008 Surface electronic structure of fcc Co films: a combined spin-resolved one- and two-photon-photoemission study *J. Phys. D: Appl. Phys.* **41** 164003
- [27] Rajeswari J, Ibach H and Schneider C M 2013 Observation of large wave vector interface spin waves: Ni(100)/fcc Co(100) and Cu(100)/Co(100) *Phys. Rev. B* **87** 235415
- [28] Steil S, Großmann N, Laux M, Ruffing A, Steil D, Wiesenmayer M, Mathias S, Monti O L A, Cinchetti M and Aeschlimann M 2013 Spin-dependent trapping of electrons at spinterfaces *Nat. Phys.* **9** 242–7
- [29] Bernien M et al 2009 Tailoring the nature of magnetic coupling of Fe-porphyrin molecules to ferromagnetic substrates *Phys. Rev. Lett.* **102** 047202
- [30] Wende H et al 2007 Substrate-induced magnetic ordering and switching of iron porphyrin molecules *Nat. Mater.* **6** 516–20
- [31] Lach S, Altenhof A, Tarafder K, Schmitt F, Ali M E, Vogel M, Sauther J, Oppeneer P M and Ziegler C 2012 Metal-organic hybrid interface states of a ferromagnet/organic semiconductor hybrid junction as basis for engineering spin injection in organic spintronics *Adv. Funct. Mater.* **22** 989–97
- [32] Djeghloul F et al 2013 Direct observation of a highly spin-polarized organic spinterface at room temperature *Sci. Rep.* **3** 1272
- [33] Javaid S et al 2010 Impact on interface spin polarization of molecular bonding to metallic surfaces *Phys. Rev. Lett.* **105** 077201
- [34] Gruber M et al 2015 Exchange bias and room-temperature magnetic order in molecular layers *Nat. Mater.* **14** 981–4
- [35] Annese E, Casolari F, Fujii J and Rossi G 2013 Interface magnetic coupling of Fe-phthalocyanine layers on a ferromagnetic surface *Phys. Rev. B* **87** 054420
- [36] Stadtmüller B, Kröger I, Reinert F and Kumpf C 2011 Submonolayer growth of CuPc on noble metal surfaces *Phys. Rev. B* **83** 085416
- [37] Van Hove M A, Koestner R J, Stair P C, Bibérian J P, Kesmodel L L, Bartoš I and Somorjai G A 1981 The surface reconstructions of the (100) crystal faces of iridium, platinum and gold *Surf. Sci.* **103** 218–38
- [38] Morgenstern K, Kibsgaard J, Lauritsen J V, Lægsgaard E and Besenbacher F 2007 Cobalt growth on two related close-packed noble metal surfaces *Surf. Sci.* **601** 1967–72
- [39] Padovani S, Scheurer F, Chado I and Bucher J P 2000 Anomalous magnetic anisotropy of ultrathin Co films grown at 30 K on Au(111) *Phys. Rev. B* **61** 72–5
- [40] Voigtländer B, Meyer G and Amer N 1991 Epitaxial growth of thin magnetic cobalt films on Au(111) studied by scanning tunneling microscopy *Phys. Rev. B* **44** 10354–7
- [41] Picone A, Riva M, Brambilla A, Giannotti D, Ivashko O, Bussetti G, Finazzi M, Ciccacci F and Duò L 2016 Atomic scale insights into the early stages of metal oxidation: a scanning tunneling microscopy and spectroscopy study of cobalt oxidation *J. Phys. Chem. C* **120** 5233–41
- [42] Cummings M, Gliga S, Lukanov B, Altman E I, Bode M and Barrera E V 2011 Surface interactions of molecular C<sub>60</sub> and impact on Ni(100) and Co(0001) film growth: a scanning tunneling microscopy study *Surf. Sci.* **605** 72–80
- [43] Cagnon L, Devolder T, Cortes R, Morrone A, Schmidt J E, Chappert C and Allongue P 2001 Enhanced interface perpendicular magnetic anisotropy in electrodeposited Co/Au(111) layers *Phys. Rev. B* **63** 104419
- [44] Donohue J 1974 *Structures of the Elements* (New York: Wiley)
- [45] Marsot N, Belkhou R, Magnan H, Le Fèvre P, Guillot C and Chandèsris D 1999 Structure and local order in Co magnetic thin films on Au(111): a surface EXAFS study *Phys. Rev. B* **59** 3135–41
- [46] Seah M P and Dench W A 1979 Quantitative electron spectroscopy of surfaces: A standard data base for electron inelastic mean free paths in solids *Surf. Interface Anal.* **1** 2–11
- [47] Davis L, MacDonald N, PalMBER P and Riach G 1987 *Handbook of Auger Electron Spectroscopy* (Eden Prairie, MN: Physical Electronics)
- [48] Speckmann M, Oepen H P and Ibach H 1995 Magnetic domain structures in ultrathin Co/Au(111): on the influence of film morphology *Phys. Rev. Lett.* **75** 2035–8
- [49] Cinchetti M, Heimer K, Wüstenberg J-P, Andreyev O, Bauer M, Lach S, Ziegler C, Gao Y and Aeschlimann M 2009 Determination of spin injection and transport in a ferromagnet/organic semiconductor heterojunction by two-photon photoemission *Nat. Mater.* **8** 115–9
- [50] Sawada M, Hayashi K and Kakizaki A 2001 Electronic structure and magnetic anisotropy of Co/Au(111): a spin-resolved photoelectron spectroscopy study *Phys. Rev. B* **63** 195407
- [51] Fujisawa H, Shiraki S, Nantoh M and Kawai M 2004 Angle-resolved photoemission study of Co nanostructures on vicinal Au(111) surfaces *Appl. Surf. Sci.* **237** 291–5
- [52] Miyamoto K, Iori K, Sakamoto K, Kimura A, Qiao S, Shimada K, Namatame H and Taniguchi M 2008 Spin-dependent electronic band structure of Co/Cu(001) with different film thicknesses *J. Phys.: Condens. Matter* **20** 225001
- [53] Himpsel F J and Eastman D E 1979 Intrinsic  $\Lambda$  1-symmetry surface state on Co(0001) *Phys. Rev. B* **20** 3217–20
- [54] Ding H F, Wulfhekel W, Henk J, Bruno P and Kirschner J 2003 Absence of zero-bias anomaly in spin-polarized vacuum tunneling in Co(0001) *Phys. Rev. Lett.* **90** 116603
- [55] Okuno S N, Kishi T and Tanaka K 2002 Spin-polarized tunneling spectroscopy of Co(0001) surface states *Phys. Rev. Lett.* **88** 066803

- [56] Aeschlimann M, Bauer M, Pawlik S, Weber W, Burgermeister R, Oberli D and Siegmann H C 1997 Ultrafast spin-dependent electron dynamics in fcc Co *Phys. Rev. Lett.* **79** 5158–61
- [57] Wüstenberg J-P, Cinchetti M, Sánchez Albaneda M, Bauer M and Aeschlimann M 2007 Spin- and time-resolved photoemission studies of thin Co<sub>2</sub>FeSi Heusler alloy films *J. Magn. Magn. Mater.* **316** e411–4
- [58] Kollamana J, Wei Z, Laux M, Stöckl J, Stadtmüller B, Cinchetti M and Aeschlimann M 2016 Scanning tunneling microscopy study of ordered C60 submonolayer films on Co/Au(111) *J. Phys. Chem. C* **120** 7568–74